STRING PERCOLATION AND THE FIRST LHC DATA*

I. Bautista[a,b], J. Dias de Deus[b], C. Pajares[a]

[a]Departamento de Física de Partículas
and
Instituto Galego de Física de Altas Enerxías
Universidade de Santiago de Compostela
15782 Santiago de Compostela, Galicia, Spain
[b]CENTRA, Departamento de Física, Instituto Superior Técnico
Av. Rovisco Pais, 1049-001 Lisboa, Portugal

(Received November 30, 2012)

The results of string percolation on multiplicities and elliptic flow in AA and pp collisions are compared with LHC data showing a good agreement. We show that the dependence of the shear viscosity over entropy density ratio on the temperature, presents a minimum close to the critical temperature remaining small in the range of the RHIC and LHC energies.

DOI:10.5506/APhysPolBSupp.6.165
PACS numbers: 25.75.–q, 25.75.Dw, 12.40.–y

1. String percolation

The percolation of strings [1–3] have described successfully the basic facts, obtained at RHIC and LHC, of the Physics of QCD matter at higher energy.

Strings are supposed to describe confined QCD interactions in an effective way. They carry color charges at the ends and an extended color field between the charges. They emit particles by string breaking and pair creation. Projected in the impact parameter they look like disks of radius $r_0 \simeq 0.2\,\mathrm{fm}$ and two-dimensional percolation theory can be applied. As the energy or the size of the projectile or target increases interaction between strings occurs due to the overlapping of the strings and the general result, due to the SU(3) random summation of color charges, is that there is a reduction in multiplicity, and an increase in the string tension of formed clusters which means an increase of $\langle p_{\mathrm{T}}^2 \rangle$.

* Presented by C. Pajares at the Light Cone 2012 Conference, Kraków, Poland, July 8–13, 2012.

The relevant variable is the transverse string density $\eta_{\rm t}$

$$\eta_{\rm t} \equiv \frac{\pi r_0^2}{S} N^{\rm s}\,, \tag{1}$$

where $N^{\rm s}$ is the number of strings and S the overlapping area. For $\eta_{\rm t}$ larger than a critical value $\eta_{\rm t}^{\rm c}$ a large cluster extends over the whole surface covering the fraction $1-e^{-\eta_{\rm t}}$ of the total area which at $\eta_{\rm t}=\eta_{\rm t}^{\rm c}$ is approximately 2/3. For homogeneous surface $\eta_{\rm t}^{\rm c}\simeq 1.2$ and for more realistic profiles $\eta_{\rm t}^{\rm c}\simeq 1.5$ [4].

The basic formulae are, for particle density [2, 3]

$$\frac{dn}{dy} = F(\eta_{\rm t}) N^{\rm s} \mu_1 \tag{2}$$

and for $\langle p_{\rm T}^2\rangle$

$$\langle p_{\rm T}^2\rangle = \frac{\langle p_{\rm T}^2\rangle_1}{F(\eta_{\rm t})}\,, \tag{3}$$

where $F(\eta_{\rm t})$ is the color reduction factor

$$F(\eta_{\rm t}) = \sqrt{\frac{1-e^{-\eta_{\rm t}}}{\eta_{\rm t}}} \tag{4}$$

and μ_1 and $\langle p_{\rm T}^2\rangle_1$ are the multiplicity and mean $p_{\rm T}^2$ produced by the fragmentation of a single string.

The multiplicity distribution can be obtained from the cluster size distribution which approximately is a gamma function and the multiplicity distribution of the cluster, which we assume Poisson like. In this way, we obtain the negative binomial distribution [5]

$$P(n,s) = \frac{\Gamma(n+k)}{\Gamma(n+1)\Gamma(k)} \frac{\gamma^k}{(1+\gamma)^{n+k}}\,, \qquad \gamma = \frac{k}{\langle n\rangle}\,, \tag{5}$$

where $\langle n\rangle$ is given by (5) and k is identical to

$$\Re \equiv \frac{\langle n(n-1)\rangle - \langle n\rangle^2}{\langle n\rangle^2} = \frac{\langle N^2\rangle - \langle N\rangle^2}{\langle N\rangle^2} = \frac{1}{k}\,, \tag{6}$$

where N is the number of effective color sources and $\Re$ the normalized two particle correlation. Since, from (3) the size area of one effective cluster $\pi r_0^2 F(\eta_{\rm t})$, and the area covered by strings is $(1-e^{-\eta_{\rm t}})\pi R^2\,\langle N\rangle$ is given by [6]

$$\langle N\rangle = \frac{(1-e^{-\eta_{\rm t}})R^2}{F(\eta_{\rm t}) r_0^2} = (1-e^{-\eta_{\rm t}})^{1/2}\sqrt{\eta_{\rm t}} \left(\frac{R}{r_0}\right)^2\,. \tag{7}$$

Note that

$$\langle N\rangle/N^{\rm s} = F(\eta_{\rm t})\,, \qquad \langle n\rangle = \langle N\rangle\mu_1\,. \tag{8}$$

We observe that in the low density limit, there is not overlapping of strings and the particle density is essentially Poisson and we have $k \to \infty$. In the large $\eta_{\rm t}$ limit, the N effective strings behave like a single string, with $\langle N^2\rangle - \langle N\rangle^2 \simeq \langle N\rangle$ and, therefore, $k \to \langle N\rangle \to \infty$. At intermediate densities, k has a minimum close to the critical $\eta_{\rm t}^{\rm c}$, k is given by [6]

$$k = \frac{\langle N\rangle}{(1-e^{-\eta_{\rm t}})^{3/2}} = \sqrt{\eta_{\rm t}}(1-e^{-\eta_{\rm t}})^{-1}\left(\frac{R}{r_0}\right)^2\,. \tag{9}$$

In the glasma picture of color glass condensate there is also obtained a negative binomial distribution. In CGC the multiplicity is given by the number of color flux tube (strings), $Q_{\rm s}^2R_A^2$, times the number of gluons produced by one, which is proportional to $1/\alpha_{\rm s}(Q_{\rm s})$. On the other hand, k is the number of flux tubes, $Q_{\rm s}^2R_A^2$, which in the limit of high density coincides with (9) having the same A and s dependencies.

Concerning the $p_{\rm T}$ distributions, assuming a Gaussian decay of each cluster, whose width is given by (3) and taking into account the gamma function distribution as the cluster size distribution we obtain the following distribution [6–9]

$$\frac{dN}{dp_{\rm T}^2dy} = \frac{dN}{dy}\frac{k'-1}{k'}\frac{F(\eta_{\rm t})}{\langle p_{\rm T}^2\rangle_1}\left(1+\frac{F(\eta_{\rm t})p_{\rm T}^2}{k'\langle p_{\rm T}^2\rangle_1}\right)^{-k'}\,. \tag{10}$$

This formula is not valid for high $p_{\rm T}$ because we have assumed a Gaussian distribution for the decay of a cluster without any power behavior corresponding to hard emissions. In (10) the k' is a function of $\eta_{\rm t}$ which has a qualitative similar dependence that k (may differ in the range of integration). At low $p_{\rm T}$, (10) behaves like $\exp(-p_{\rm T}^2/\langle p_{\rm T}^2\rangle)$ and at moderate $p_{\rm T}$ has a power-like behavior. The formula (10) is valid at all energies and centralities including pp collisions, and gives a right description of RHIC and LHC data, up to $p_{\rm T} \simeq 5\,{\rm GeV}/c$.

Note that at low energy density (10) behaves like $\exp(-p_{\rm T}^2/\langle p_{\rm T}^2\rangle_1)$. As the energy density increases, k' decreases and there is a departure of the exponential behavior. However, above the critical point k' increases again and the exponential behavior is recovered.

2. Multiplicity distributions

The new LHC data has shown that the multiplicity at central rapidity rises faster in central Pb–Pb collisions than in pp collisions. On the other hand, the data show the dependence in the centrality of the multiplicity in AA is the same at LHC and RHIC energies. These two facts are explained in our approach.

The apparently different behavior of the multiplicities is due to energy conservation. In fact, in Pb–Pb collisions the number of strings grows like the number of collisions, $N_A^{4/3}$, and only the energy available grows like A. Therefore, at not very high energy, there will be strings that cannot be formed because there is not energy available. We take into account this effect assuming that the number of strings increases like $N_A^{1+\alpha(\mathrm{s})}$, where $\alpha(\mathrm{s})$ is 0 at low energy and goes to 1/3 at very high energy. In this way, we obtain [10]

$$\left.\frac{1}{N_A}\frac{dn}{y}\right|_{N_AN_A} = \kappa \left.\frac{dn}{dy}\right|_{pp} \left[1 + \frac{F\left(\eta^{\mathrm{t}}_{N_A}\right)}{F\left(\eta^{\mathrm{t}}_{p}\right)}\left(N_A^{\alpha(\mathrm{s})} - 1\right)\right], \tag{11}$$

with

$$\eta^{\mathrm{t}}_{N_A} = \eta^{\mathrm{t}}_p N_A^{\alpha}\left(\frac{A}{N_A^{2/3}}\right), \qquad \alpha = \frac{1}{3}\left(1 - \frac{1}{1+\ln\left(\sqrt{s/s_0}+1\right)}\right) \tag{12}$$

and

$$\left.\frac{dn}{dy}\right|_{pp} = a\left(\frac{s}{m_p}\right)^{\lambda/2}. \tag{13}$$

In Fig. 1, we show our results with the parameters $\kappa = 0.63 \pm 0.01$, $\lambda = 0.201 \pm 0.003$, and $\sqrt{s_0} = 245 \pm 29\,\mathrm{GeV}$, $\lambda = 0.23$ together with the data for AA and pp [11]. In Fig. 2, we show our results concerning the centrality dependence for Pb–Pb at LHC energy and Cu–Cu and Au–Au at RHIC energy.

Concerning the rapidity dependence, there is not limiting fragmentation scaling in the percolation approach [12] and the evolution with energy is very different for different values of the pseudorapidity η. We obtain a very good description of pp and AA at all energies and centralities including the TOTEM data of high pseudorapidity [13, 14].

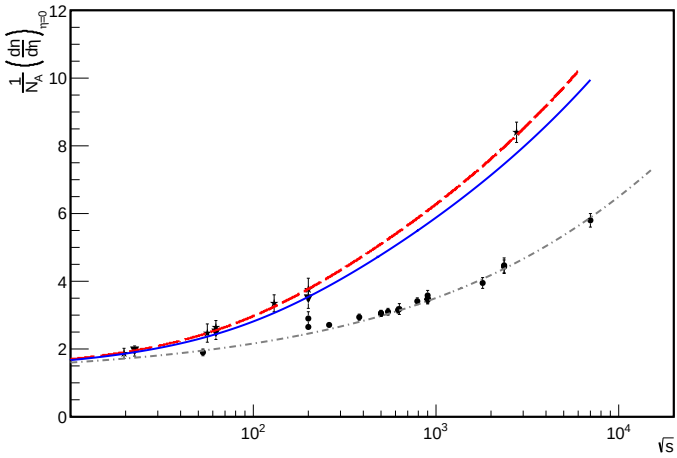

Fig. 1. (Color online) Multiplicity dependence on p, s, pp data (circles), CuCu (triangles) and AuAu and PbPb (stars) [12], $dN_{\rm ch} = d$ form formula (11) ($N_A = 1$, $A = 1$) for pp (dashed-dotted/grey line); ($N_A = 50$, $A = 63$) for CuCu (solid/blue line); and ($N_A = 175$, $A = 200$) for AuAu/PbPb (dashed/red line).

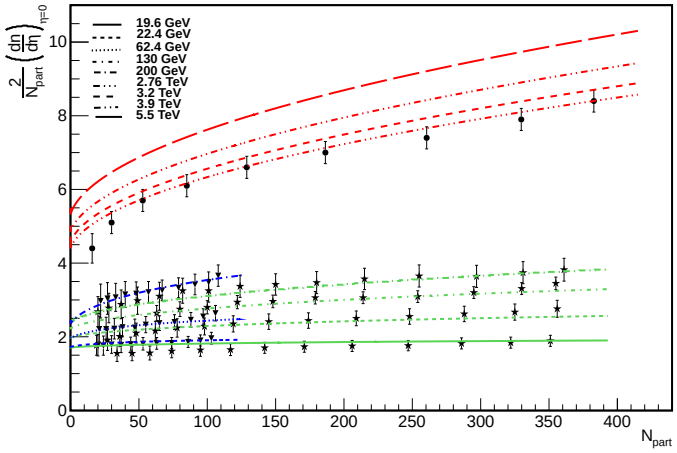

Fig. 2. (Color online) Multiplicity dependence on centrality (the number of participating nucleons $N_{\rm part} = 2N_A$, where N_A is the number of participants per nucleus). CuCu (triangles) and AuAu (stars) data, PbPb (circles). Curves obtained from (11) ($\sqrt{s} = 22.4$, 62.4, 200 GeV) for CuCu (blue lines); ($\sqrt{s} = 19.6$, 62.4, 130, 200 GeV) for AuAu (green lines); and ($\sqrt{s} = 2.76$, 3.2, 3.9, 5.5 TeV) for PbPb (red lines).

3. Elliptic flow

In a precisely $b = 0$, in AA or pp collisions the projected area in the impact parameter plane is a circle populated by disks approximately in a azimuthal uniform way. If $b \neq 0$, we have a projected almond. If we imagine the projected almond to be obtained by a deformation of the circle, it is clear that the string density is larger along the smaller, x axis, than the density along the y axis. It is intrinsic anisotropy that determines the existence of elliptic flow v_2. Also energy loss arguments support an sizable v_2 [14, 15]. Notice that in percolation we have in the initial state interactions of the partons of the individual strings as a consequence of the color arrangement which is produced inside the formed cluster. The fragmentation of this large cluster produces a thermal distribution of particles [16] and provide us the required early thermalization as far as the fragmentation time is around 1 fm.

In order to compute v_2, we introduce the transverse azimuthal density [15, 17–19]

$$\eta_\phi^{\mathrm{t}} = \eta^{\mathrm{t}} \left(\frac{R}{R_\phi} \right)^2 , \tag{14}$$

where

$$R_\phi = R_A \frac{\sin(\phi - \alpha)}{\sin \phi} , \tag{15}$$

$$\alpha = \sin^{-1} \left(\frac{b}{2R_A} \sin \phi \right) \tag{16}$$

and

$$\frac{\pi R_A^2}{4} \simeq \frac{1}{2} \int_0^{\pi/2} d\phi dR_\phi^2 . \tag{17}$$

Introducing (15) into the transverse momentum distribution (10) and expanding the resulting distribution in powers of $(R_\phi^2 - R^2)$, retaining the first two terms, we obtain

$$\begin{aligned} v_2(p_{\mathrm{T}}^2, y) = & \left[\frac{2}{\pi} \int_0^{\pi/2} d\phi \cos 2\phi \left(\frac{R_\phi}{R} \right)^2 \right] \\ & \times \left(\frac{e^{-\eta^{\mathrm{t}}} - F(\eta^{\mathrm{t}})^2}{2F(\eta^{\mathrm{t}})} \right) \frac{F(\eta^{\mathrm{t}}) p_{\mathrm{T}}^2 / \langle p_{\mathrm{T}}^2 \rangle_1}{\left(1 + F(\eta^{\mathrm{t}}) p_{\mathrm{T}}^2 / \langle p_{\mathrm{T}}^2 \rangle_1\right)} . \end{aligned} \tag{18}$$

We observe that at low p_{T} the dependence on η^{t} is given by $(e^{-\eta^{\mathrm{t}}} - F^2(\eta^{\mathrm{t}}))/2F(\eta^{\mathrm{t}})$ which remain approximately constant for the values of η^{t} corresponding to RHIC and LHC.

In Fig. 3, we compare our results on the dependence of v_2 on $p_{\rm T}$ with RHIC and LHC data at different centralities [20].

We also reproduce the centrality dependence of the data as well as the π, κ and p v_2 [16–18, 21]. We are able to obtain a good description of the data on higher harmonics [14]. Notice that our results are obtained from a close analytical universal formula valid for all centralities, energies, projectiles and targets.

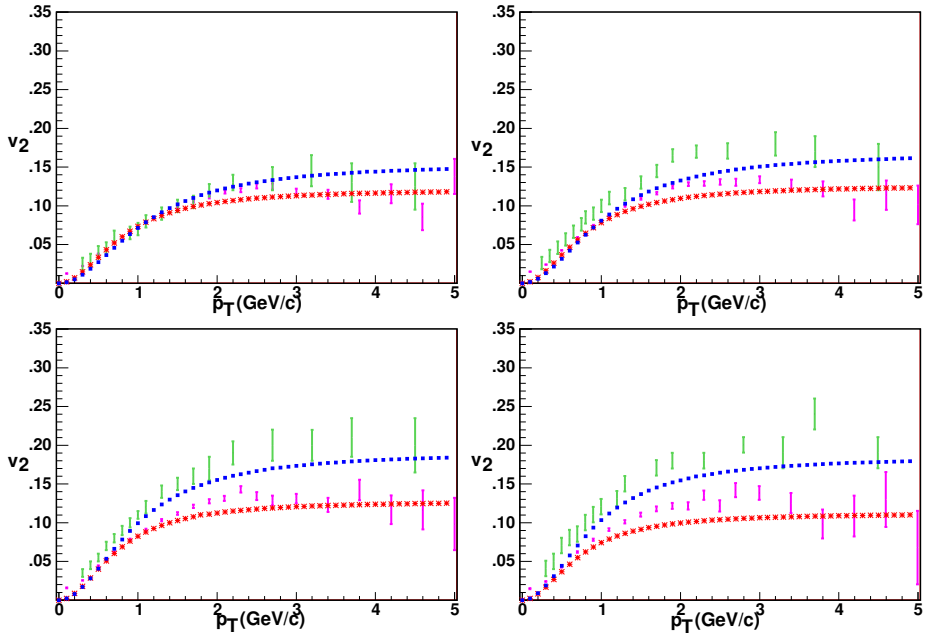

Fig. 3. (Color online) Stars (red) and squares (blue) correspond to our predictions for $\sqrt{s} = 200\,\text{GeV}$ and $\sqrt{s} = 2.76\,\text{TeV}$ energies, and upper (green) and lower (pink) error-bars are the respective data from RHIC and LHC for centralities 10–20%, 20–30%, 30–40%, 40–50% [20], figure caption order from top left to bottom right respectively.

4. Shear viscosity entropy density ratio

The shear viscosity to entropy density ratio is a measured of the fluidity and the RHIC and LHC data show a low value, lower than most of the known substances. In string percolation we obtain also a low η/s [22]. In fact, in percolation the strong color field inside the large cluster produces deacceleration which can be seen as a thermal temperature [16, 19] by means of Hawking–Unruh effect. The temperature is given by

$$T\left(\eta^{\rm t}\right) = \sqrt{\left\langle p_{\rm T}^2 \right\rangle_1 / 2F\left(\eta^{\rm t}\right)}\,. \tag{19}$$

On the other hand, from the relativistic kinetic theory η/s is given by

$$\frac{\eta}{s} = \frac{T\lambda}{5} = \frac{1}{n\sigma_{\rm tr}}\,, \tag{20}$$

where λ is the mean free path, n the number density and $\sigma_{\rm tr}$ the transport cross section.

From equation (7), we have

$$n = \frac{1 - e^{-\eta^{\rm t}}}{\pi r_0^2 F(\eta^{\rm t}) L} \tag{21}$$

and

$$\sigma_{\rm tr} = S_1 F\left(\eta^{\rm t}\right) = \frac{\pi r_0^2 \left\langle p_{\rm T}^2 \right\rangle_1}{2T^2}\,. \tag{22}$$

From (21) and (22), we obtain

$$\frac{\eta}{s} = \frac{L\sqrt{\left\langle p_{\rm T}^2 \right\rangle_1}\eta_{\rm t}^{1/4}}{5\sqrt{2}(1 - e^{-\eta_{\rm t}})^{5/4}}\,. \tag{23}$$

In Fig. 4, we show η/s as a function of $T/T_{\rm c}$. Close to the critical temperature presents a minimum and remains small in the RHIC and LHC range growing slowly.

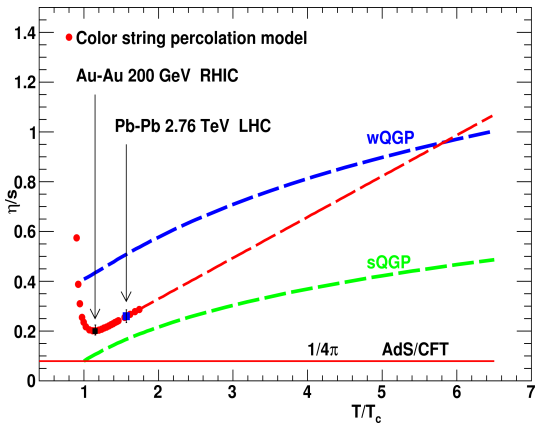

Fig. 4. η/s as a function of $T/T_{\rm c}$.

We thank J.G. Milhano, A.S. Hirsch, R.P. Scharenberg and B. Srivastava who have collaborated in part of the work reported here. We thank the support of the FCT/Portugal project PPCDT/FIS/5756682004, the project FPA2011-22776 of MICINN of Spain, the Consolider project and the conselleria Eduacion da Xunta de Galicia.

REFERENCES

[1] N. Armesto, M.A. Braun, E.G. Ferreiro, C. Pajares, *Phys. Rev. Lett.* **77**, 3736 (1996); M. Nardi, H. Satz, *Phys. Lett.* **B442**, 14 (1998).

[2] M.A. Braun, C. Pajares, *Phys. Rev. Lett.* **85**, 4864 (2000); M.A. Braun, C. Pajares, *Eur. Phys. J.* **C16**, 349 (2000).

[3] M.A. Braun, F. Del Moral, C. Pajares, *Phys. Rev.* **C65**, 024907 (2002).

[4] A. Rodrigues, R. Ugoccioni, J. Dias de Deus, *Phys. Lett.* **B458**, 402 (1999).

[5] J. Dias de Deus, E.G. Ferreiro, C. Pajares, R. Ugoccioni, *Eur. Phys. J.* **C40**, 229 (2005).

[6] J. Dias de Deus, C. Pajares, *Phys. Lett.* **B695**, 211 (2011).

[7] L. Cunqueiro, J. Dias de Deus, E.G. Ferreiro, C. Pajares, *Eur. Phys. J.* **C53**, 585 (2008).

[8] C. Pajares, *Eur. Phys. J.* **C43**, 9 (2005).

[9] J. Dias de Deus, R. Ugoccioni, *Eur. Phys. J.* **C43**, 249 (2005).

[10] I. Bautista, J. Dias de Deus, J.G. Milhano, C. Pajares, *Phys. Lett.* **B715**, 230 (2012).

[11] UA1 Collaboration, *Nucl. Phys.* **B335**, 261 (1990); G.J. Alner *et al.* [UA5 Collaboration], *Phys. Rep.* **154**, 247 (1987); STAR Collaboration, *Phys. Rev.* **C79**, 034909 (2009); CDF Collaboration, *Phys. Rev.* **D41**, 2330 (1990); K. Aamodt *et al.* [ALICE Collaboration], *Eur. Phys. J.* **C68**, 89 (2010); V. Khachatryan *et al.* [CMS Collaboration], *J. High Energy Phys.* **1002**, 041 (2010); V. Khachatryan *et al.* [CMS Collaboration], *Phys. Rev. Lett.* **105**, 022002 (2010); B. Alver *et al.* [PHOBOS Collaboration], *Phys. Rev.* **C83**, 024913 (2011); K. Aamodt *et al.* [ALICE Collaboration], *Phys. Rev. Lett.* **106**, 032301 (2011).

[12] P. Brogueira, J. Dias de Deus, C. Pajares, *Phys. Rev.* **C75**, 054908 (2007).

[13] I. Bautista, C. Pajares, J. Dias de Deus, *Nucl. Phys.* **A882**, 44 (2012); I. Bautista, C. Pajares, J.G. Milhano, J. Dias de Deus, *Phys. Rev.* **C86**, 034909 (2012).

[14] M.A. Braun, C. Pajares, V.V. Vechernin, `arXiv:1204.5829 [hep-ph]`.

[15] M.A. Braun, C. Pajares, *Eur. Phys. J.* **C71**, 1549 (2011).

[16] J. Dias de Deus, C. Pajares, *Phys. Lett.* **B642**, 455 (2006).

[17] I. Bautista, J. Dias de Deus, C. Pajares, *Phys. Lett.* **B693**, 362 (2010).

[18] I. Bautista, J. Dias de Deus, C. Pajares, *Eur. Phys. J.* **C72**, 2038 (2012).

[19] D. Kharzeev, E. Levin, K. Tuchin, *Phys. Rev.* **C75**, 044903 (2007); P. Castorina, D. Kharzeev, H. Satz, *Eur. Phys. J.* **C52**, 187 (2007).

[20] K. Aamodt *et al.* [ALICE Collaboration], *Phys. Rev. Lett.* **105**, 252302 (2010); B.B. Back *et al.* [PHOBOS Collaboration], *Phys. Rev.* **C65**, 061901 (2002); S. Manly *et al.* [PHOBOS Collaboration], *Nucl. Phys.* **A774**, 523 (2006).

[21] I. Bautista, L. Cunqueiro, J.D. de Deus, C. Pajares, *J. Phys. G* **37**, 015103 (2010).

[22] J.D. de Deus *et al.*, *Eur. Phys. J.* **C72**, 2123 (2012).